PROCEEDINGS B

royalsocietypublishing.org/journal/rspb

Research

Cite this article: Neto-Bradley BM, Muir CD, Whitton J, Pennell MW. 2021 Phylogenetic history of vascular plant metabolism revealed using a macroevolutionary common garden. *Proc. R. Soc. B* **288**: 20210605.
https://doi.org/10.1098/rspb.2021.0605

Received: 23 October 2020
Accepted: 7 May 2021

Subject Category:
Evolution

Subject Areas:
evolution, plant science

Keywords:
macroevolution, plant metabolism, photosynthesis, botanical garden, V_{cmax}, J_{max}

Authors for correspondence:
Barbara M. Neto-Bradley
e-mail: barbaranetobradley@gmail.com
Matthew W. Pennell
e-mail: pennell@zoology.ubc.ca

Electronic supplementary material is available online at https://doi.org/10.6084/m9.figshare.c.5426556.

THE ROYAL SOCIETY PUBLISHING

Phylogenetic history of vascular plant metabolism revealed using a macroevolutionary common garden

Barbara M. Neto-Bradley[1,2], Christopher D. Muir[4], Jeannette Whitton[1,2] and Matthew W. Pennell[2,3]

[1]Department of Botany, [2]Biodiversity Research Centre, and [3]Department of Zoology, University of British Columbia, Vancouver, Canada
[4]School of Life Sciences, University of Hawai'i, Honolulu, HI, USA

BMN-B, 0000-0002-6061-208X; CDM, 0000-0003-2555-3878; JW, 0000-0003-1609-5203

While the fundamental biophysics of C_3 photosynthesis is highly conserved across plants, substantial leaf structural and enzymatic variation translates into variability in rates of carbon assimilation. Although this variation is well documented, it remains poorly understood how photosynthetic rates evolve, and whether macroevolutionary changes are related to the evolution of leaf morphology and biochemistry. A substantial challenge in large-scale comparative studies is disentangling evolutionary adaptation from environmental acclimation. We overcome this by using a 'macroevolutionary common garden' approach in which we measured metabolic traits (J_{max} and V_{cmax}) from 111 phylogenetically diverse species in a shared environment. We find substantial phylogenetic signal in these traits at moderate phylogenetic timescales, but this signal dissipates quickly at deeper scales. Morphological traits exhibit phylogenetic signal over much deeper timescales, suggesting that these are less evolutionarily constrained than metabolic traits. Furthermore, while morphological and biochemical traits (LMA, N_{area} and C_{area}) are weakly predictive of J_{max} and V_{cmax}, evolutionary changes in these traits are mostly decoupled from changes in metabolic traits. This lack of tight evolutionary coupling implies that it may be incorrect to use changes in these functional traits in response to global change to infer that photosynthetic strategy is also evolving.

1. Introduction

Patterns of trait variation within and across species may be very different when examined at different scales [1], and these differences can provide key insights into the nature of selection and constraints that act upon these traits [2–4], complementing insights gleaned from individual experimental studies [5]. Additionally, evaluating the phylogenetic history of trait variation can help researchers make predictions about phenotypes that are difficult to measure but which may be crucial for conservation and ecological modelling [6]. While we currently understand a great deal about the macroevolutionary history of plant 'functional traits' [7–9], the broad-scale evolutionary dynamics of photosynthetic capacity have focused nearly exclusively on transitions from C_3 to C_4 [10] rather than on variation within the predominant C_3 mode (but see [11–13]). This knowledge gap is especially notable given the well-characterized biophysics of C_3 photosynthesis [14,15], and how many studies have examined genetic and environmental sources of variation [16,17] in these traits within and between species.

Here, we address this gap by quantifying variation in parameters of the Farquhar–von-Caemmerer–Berry (FvCB) biophysical model of C_3 photosynthesis [14,15]. Specifically, we focus on two key metabolic traits: V_{cmax}, which describe the maximum rate of carboxylation and J_{max}, the maximum rate of electron transport. Both traits are estimated from fitting the FvCB model to A-C_i curves that describe the photosynthetic assimilation rate A as a function of

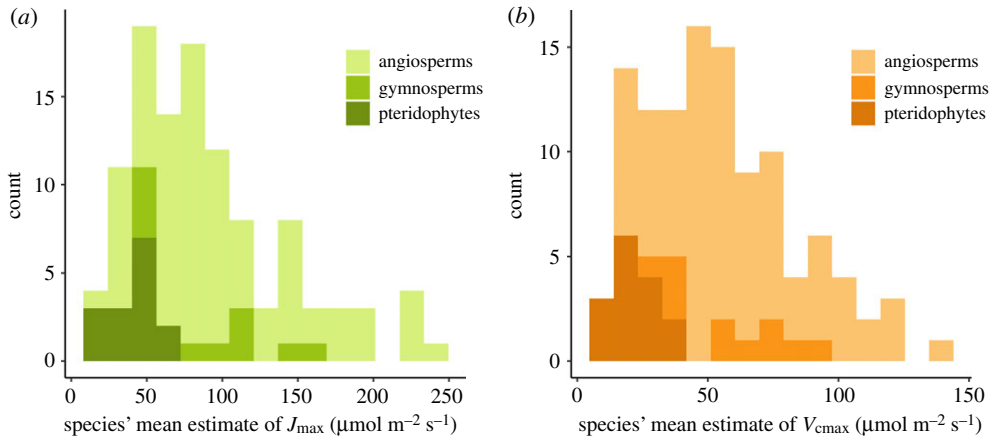

Figure 1. Histogram of the J_{max} (*a*) and V_{cmax} (*b*) estimates from our macroevolutionary common garden. Species of angiosperms ($n = 85$) are shaded in the lightest colour, followed by gymnosperms ($n = 11$) shaded in a darker colour and pteridophytes ($n = 15$), shaded in the darkest colour. (Online version in colour.)

internal leaf carbon dioxide concentration (C_i) [18]. There is evidence that there are differences in the parameters of photosynthesis models between major groups (i.e. angiosperms, gymnosperms and pteridophytes [19–22]). But current knowledge is insufficient to bridge the observations of broad-scale phylogenetic variation with abundant evidence of local (evolutionary) adaptation and (physiological) acclimation in these traits [23–26]; what is needed is comparative data collected across multiple evolutionary scales.

As noted above, photosynthetic traits have been measured in thousands of studies and efforts have been made to compile these data [16,21,27]. While these compilations can provide insights into some broad questions such as how plants might respond to elevated temperature and CO_2 [28], they are of limited value for addressing evolutionary questions because the signal of interspecific variation is confounded with differences in measurement procedures and with responses to local environmental conditions [16].

We take what we call a *macroevolutionary common garden* approach: we measured species from across the plant tree of life in a single season in two nearby botanical gardens—the University of British Columbia Botanical Garden and the VanDusen Botanical Garden, both in Vancouver, Canada—using standardized protocols and taking measurements under a restricted set of conditions, allowing us to reduce variation due to environmental and methodological noise. We recognize that the species that can grow in southwestern Canada are a non-random subset of all plant species, leading us to focus here on broad-scale patterns and results. We used the recently developed Rapid A-C_i (RACiR) [29] method coupled with technological advances in gas exchange measurement equipment and repeatedly measured our broad sample of species over a single field season, which also mitigated extraneous sources of variability. For each individual plant, we collected A-C_i curves and measured conventional 'functional' traits including leaf area, leaf mass per area, and nitrogen and carbon concentrations per area (N_{area} and C_{area}), repeating this sampling three times over the growing season. Taking all of our measurements on the same leaf allowed us to avoid introducing the well-documented substantial variation in morphological and metabolic traits among leaves even within a single plant [30] and preserve potential patterns of covariation among traits. In total, after quality-control steps (Methods) the final dataset contained 111 species. We then paired our measurements with the megaphylogeny of Zanne *et al*. [9] to investigate the macroevolutionary history of photosynthetic capacity and to test for correlated evolution with morphological and biochemical phenotypes.

2. Results and Discussion

The plants in our macroevolutionary common garden exhibit substantial variation in photosynthetic capacity as measured by differences in the means and variances of J_{max} and V_{cmax} between major plant groups, consistent with previous results [19–21]. Within angiosperms, estimates of J_{max} range from 17.70 to 240.00 µmol m^{-2} s^{-1} and for V_{cmax}, from 14.10 to 139.00 µmol m^{-2} s^{-1}. This range is broader than that of pteridophytes ($J_{max} = 14.20$–64.70 µmol m^{-2} s^{-1}; $V_{cmax} = 9.09$–36.60 µmol m^{-2} s^{-1}) or gymnosperms ($J_{max} = 45.30$–169.00 µmol m^{-2} s^{-1}; $V_{cmax} = 27.20$–88.40 µmol m^{-2} s^{-1}) (figure 1). Means and variances are significantly different among lineages for both J_{max} (Kruskal–Wallis test: $\chi^2 = 25.554$, d.f. = 2, $p < 0.001$; Levene's test: $F = 6.2075$, d.f. = 2, $p = 0.0028$) and V_{cmax} (Kruskal–Wallis test; $\chi^2 = 27.200$, d.f. = 2, $p < 0.001$; Levene's test: $F = 7.198$, d.f. = 2, $p = 0.0012$). This is further illustrated when we plot J_{max} and V_{cmax} values on a phylogeny (figure 2; electronic supplementary material, figures S1 and S2). For example, pteridophytes exhibit lower trait values with less variation than those of angiosperms and gymnosperms (figure 2).

To gain deeper insights into evolutionary processes acting across timescales, we fit phylogenetic models to our metabolic and functional traits. Specifically, we fit a model of adaptation and constraint [31] and estimated the 'phylogenetic half-life' [32] using maximum likelihood. Phylogenetic half-life measures how quickly the history of trait change is erased by subsequent evolution and contemporary environmental variation. A relatively short half-life is inferred when close relatives often differ from each other in trait values, whereas a very long half-life is consistent with gradual accumulation of variation over time. Both J_{max} and V_{cmax} had moderate phylogenetic half-lifes (maximum-likelihood estimates (MLE) of 76 million years (Ma), 106 Ma, respectively, relative to a tree age of approximately 390 Ma; figure 3). This means that over these timescales, the metabolic traits of a species (growing under conditions similar to ours)

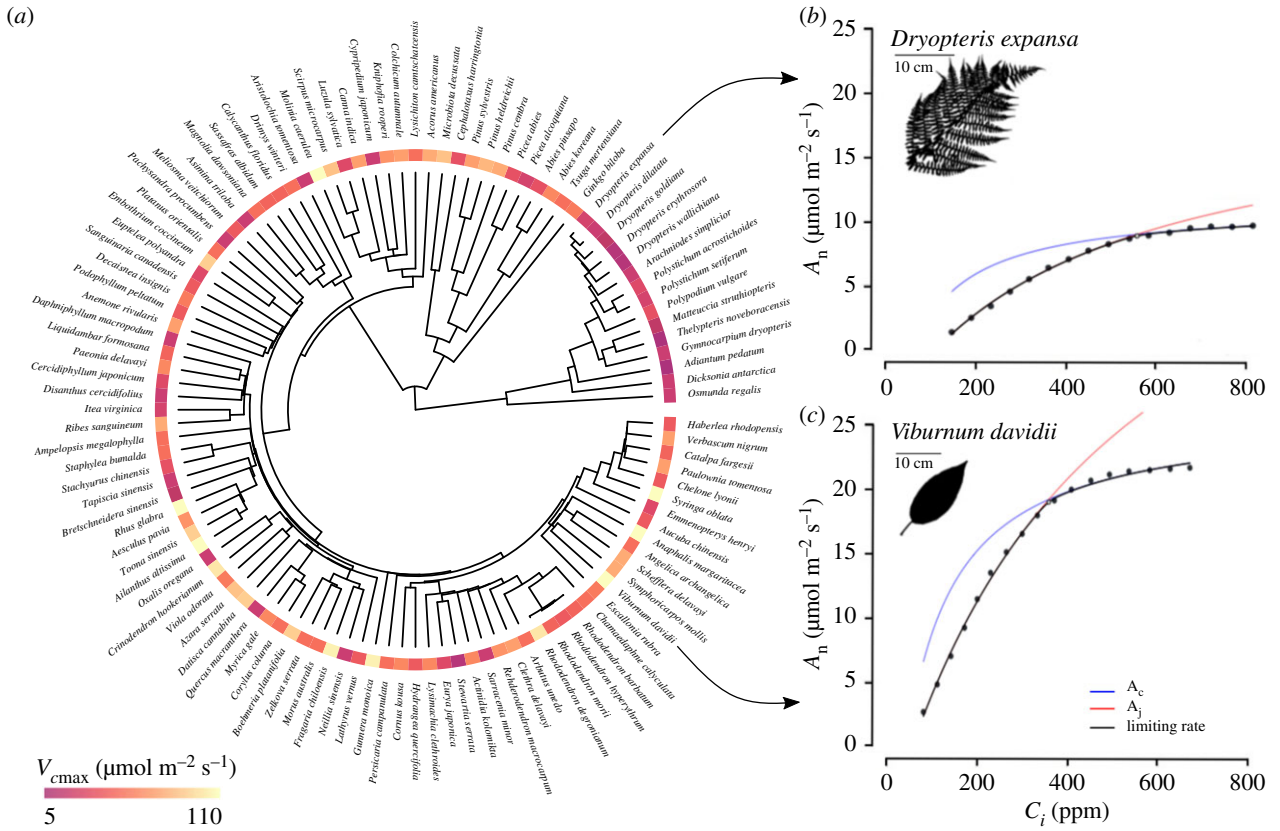

Figure 2. Part (*a*) illustrates the pruned vascular plant phylogeny of 111 species, depicting the structure of species' mean V_{cmax} estimates from our macroevolutionary common garden. Low V_{cmax} estimates are shown in dark shades and high values in light shades. Two examples of the RACiR curves these estimates are derived from are shown on the right; for (*b*) *Dryopteris expansa*'s low V_{cmax} estimate and (*c*) *Viburnum davidii*'s high estimate. The illustrated *D. expansa* and *V. davidii* leaves are scans of leaves measured in our macroevolutionary common garden. (Online version in colour.)

are well predicted from those of its close relatives. This remarkable finding suggests that these metabolic traits show the signature of their evolutionary history, despite fundamental constraints on the range of variability (which are manifested in the dissipation of phylogenetic information at timescales beyond approx. 100 MYA). At a practical level, this also means that, with some caveats, it seems plausible that researchers could impute metabolic data for data deficient species.

Morphological traits have even longer phylogenetic half-lives than metabolic traits (MLE of 240 Ma for leaf mass and 707 Ma for leaf area; figure 3). At the other end of the spectrum, biochemical traits have much shorter phylogenetic half-lives (MLE of 2 Ma for C_{area} and 39 Ma for N_{area}) than these previous traits. This lack of deep phylogenetic signal suggests that trait values are constrained such that species differences essentially represent 'evolutionary noise' with lineages repeatedly shifting among states over time. Notably, we found that leaf morphological trait variance accumulates in a Brownian motion-like fashion, which seems highly unlikely if our sampling was biased towards convergently evolved phenotypes. Since it is not clear to us why we would expect the metabolic measurements to be even more biased towards convergence than the leaf phenotypes themselves, we have reason to believe that both the estimated rates and the inferred ability to impute should be quite general. Although we argue for the generality of our findings, we recognize that our results could be impacted by the specific conditions of the coastal temperate environment in which we conducted our study; we eagerly await further validation using data from comparable studies in different climatic regions.

We find limited evidence that metabolic traits are co-evolving with the plant functional traits we studied. While the coevolution of metabolic processes and organismal attributes has been extensively examined in animals [33,34], it remains underexplored in plants (but see [35]), particularly at large scales. We know from work on the leaf economics spectrum [36] that maximum photosynthetic rate (often denoted A_{max}) covaries with many plant functional traits. Previous work also links J_{max} and V_{cmax} to N_{area}, due to high leaf nitrogen investment in ribulose-1,5-bisphosphate oxygenase/carboxylase (RuBisCO) [16]. When we use phylogenetic linear models to predict either J_{max} or V_{cmax} using leaf mass per area (LMA; the ratio of mass/area used here to avoid spurious correlations [37]), N_{area}, C_{area} and species' identity, only N_{area} is a significant predictor of J_{max} ($\beta_{LMA} = -4601.38$, $p_{LMA} = 0.088$, $\beta_{N\,area} = 694.25$, $p_{N\,area} = 0.015$, $\beta_{C\,area} = 102.58$, $p_{C\ area} = 0.058$; electronic supplementary material, table S1), while both N_{area} and C_{area} show a significant relationship with V_{cmax} ($\beta_{LMA} = -2825.37$, $p_{LMA} = 0.056$, $\beta_{N\,area} = 376.63$, $p_{N\,area} = 0.015$, $\beta_{C\,area} = 61.27$, $p_{C\,area} = 0.040$; electronic supplementary material, table S2).

In addition to tests for correlated evolution of *states* (the measured phenotype), we tested for correlations in *rates* of trait evolution, i.e. whether rapid evolution in one trait was associated with rapid evolution in other traits (for discussion of this distinction, see [38]). To test for rate correlations, we computed independent contrasts [39] at each node, then took the logarithm of the absolute value of these contrasts as our estimate of the local rate of evolution [40]. We then tested for correlations between these node-specific rate estimates for all pairs of traits. Despite evidence of pairwise

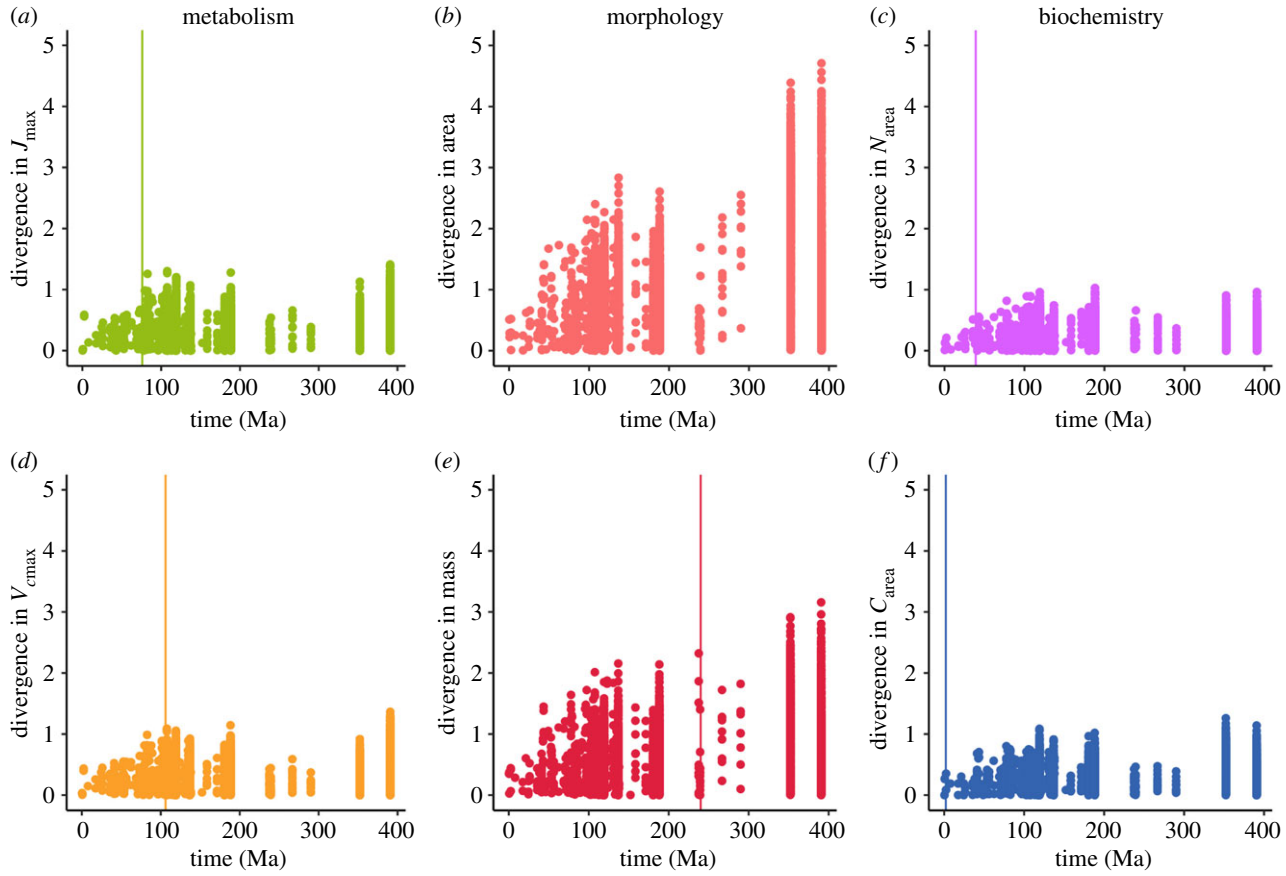

Figure 3. Divergence through time plots of (*a*) J_{max}, (*b*) leaf area, (*c*) N_{area}, (*d*) V_{cmax}, (*e*) leaf mass and (*f*) C_{area}. Divergence is the log difference between two trait values, corrected by their dimensionality (i.e. whether these are mass, area or linear based measurements). The absolute values of divergence (a unitless measure) are plotted along the *y*-axis, and time, measured in millions of years (Ma) is plotted on the *x*-axis. Using our novel 'macroevolutionary common garden' dataset, containing trait data on 111 species, each point depicts the absolute value of the estimated trait divergence between two taxa drawn from our dataset. Each divergence estimate is plotted against the time since two species shared a common ancestor (i.e. time since MRCA) in Ma. The vertical line in each panel depicts the estimated phylogenetic half-life for that trait. The half-life estimate for area (707 Ma) is omitted from (*b*) for visual ease. (Online version in colour.)

correlations in both trait values and rates of evolution in our suite of trait combinations (Pearson correlation coefficient $r > 0.5$ for four of 10 trait combinations; figure 4), there is a notable lack of correspondence between the rates of evolution of metabolic traits J_{max} or V_{cmax} and the remainder of our traits ($r > 0.5$ for only two of 10 rate combinations; figure 4). This indicates that while morphological and biochemical traits are broadly predictive of metabolic traits (J_{max} and V_{cmax}) in the present (electronic supplementary material, tables S1 and S2), the rates of evolution of these traits are decoupled over deeper evolutionary timescales.

Our results highlight a fundamental mismatch: metabolic traits and functional traits have distinct evolutionary dynamics. Specifically, we show that (i) the morphological traits that we measured show little evidence of constrained evolution, while biochemical traits are more constrained than our metabolic traits; (ii) measured functional traits are not tightly correlated with specific metabolic traits over evolutionary time and (iii) there is little correlation in branch-wise rates of evolution between the different classes of traits. This decoupling is critical to appreciate and suggests caution when using changes in functional traits as proxies for metabolic responses. As plants evolve and adapt under anthropogenic climate change, the evolutionary responses of specific functional and metabolic traits may not be correlated.

Many among-species trait correlations are not recapitulated within species, indicating that macroevolutionary patterns do not emerge from fundamental structure–function relationships or genetic correlations [41]. Furthermore, we show that among-species trait correlations do not necessarily arise from shared macroevolutionary dynamics; therefore, shifts in functional traits may not be predictive of shifts in metabolic traits. The phylogenetic perspective provided by our analysis provides a richer understanding of the evolutionary constraints and selection pressures operating on metabolic traits and suggests new ways to both look back and to look forward. It is now possible, for instance, to use the estimated macroevolutionary rates in conjunction with contemporary data to reconstruct historical physiologies; such an approach could be used to understand how these traits have evolved in response to palaeo-environments [42,43]. We also suggest that better incorporation of variation in metabolic traits into Earth System Models may improve the accuracy of model predictions [44]. Furthermore, since we have shown that J_{max} and V_{cmax} have substantial phylogenetic signal at shallow scales, reliably imputing values of these traits for ecologically important but data deficient species is likely feasible, though more work is needed to validate these use cases. While large-scale efforts are now focused on engineering crop plants with more efficient photosynthetic traits [45], our results suggest that substantial unexplored variation may mean that more efficient traits can be 'borrowed' from closer evolutionary relatives, with the search guided by large-scale phylogenetic comparative

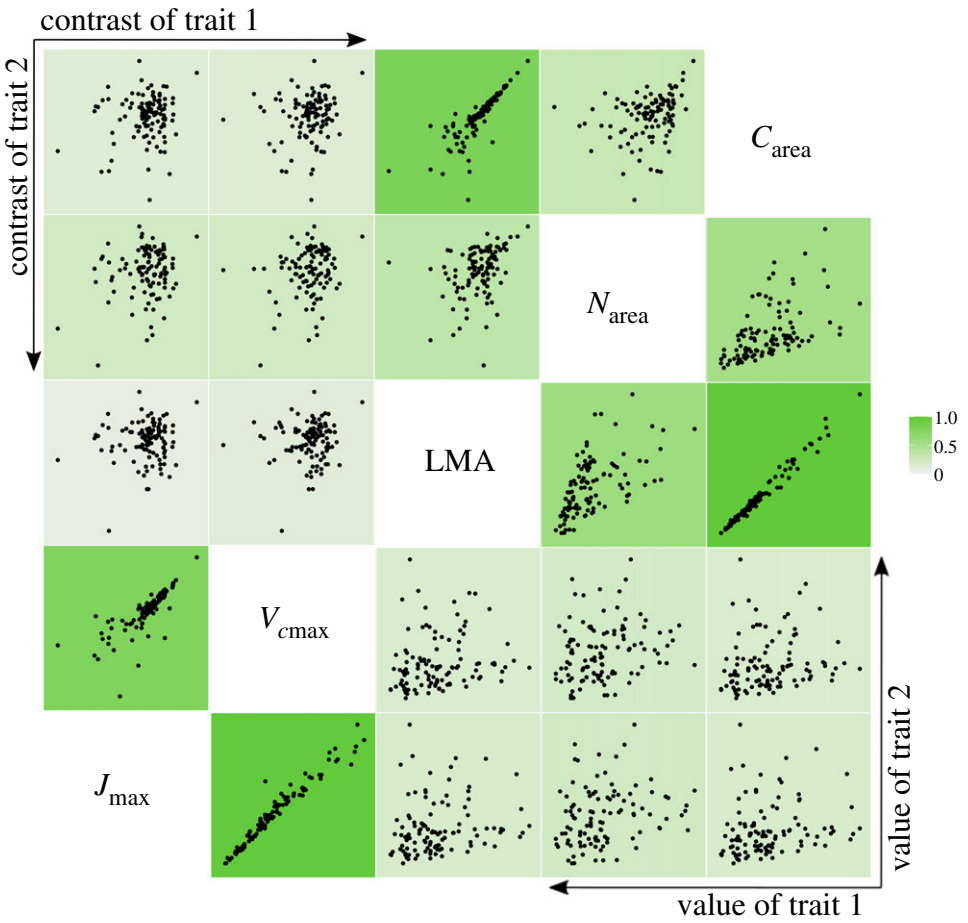

Figure 4. Scatter plots of all pairwise combinations of the PICs for J_{max}, V_{cmax}, LMA, N_{area} and C_{area} (above the diagonal), and of trait values (below the diagonal). The background of each scatter plot is coloured corresponding to the strength of the correlation between each pair of values. None of the correlations was negative. (Online version in colour.)

analyses such as ours. More broadly we argue that despite being widely measured, the variation and phylogenetic structure in C_3 photosynthesis is understudied relative to its potential value to contribute to both our understanding of impacts, and to providing solutions to address the challenges of anthropogenic climate change.

3. Methods

(a) Species selection

We sampled 111 species across the tree of vascular plants. Working from the intersection of the species in the Zanne *et al.* phylogeny of plants and the lists of species growing at the UBC Botanical Garden (49.253841° N, 123.251101° W) and VanDusen Botanical Garden (49.2394° N, 123.1289° W), we randomly selected one species from each family represented in either garden for inclusion in our study. In addition, in order to quantify differences in traits among more recently diverged taxa, we sampled a further 6–8 species from one family of ferns, conifers and angiosperms (Dryopteridaceae, Pinaceae and Ericaceae, respectively). This approach to selecting species allowed us to cover a range of divergence times between taxa. Although this sampling is taxonomically biased, we note that none of the phylogenetic methods that we used assume that lineages are sampled in proportion to their true diversity.

For each species, a single individual was selected from the botanical gardens, with each of the traits described below (RACiR, leaf area and leaf mass) measured three times for each plant, once in each of three rounds of sampling that occurred between 6 May and 18 July 2019. Although we acknowledge that there are differences in light, temperature, water and nutrients both between and within each of the gardens, this environmental variation is random with respect to plant relationships. Further, within each round, we randomized the order in which species were sampled in order to reduce the effects of day-to-day and seasonal variation on measurements. As such, the effects of this variation are likely greatly reduced relative to studies that compile data from various sources and locations.

(b) Photosynthesis data

We measured metabolic traits using a recently developed rapid A-C_i response (RACiR) [29] approach. This allows us to measure A-C_i response curves in under 15 min, far less than the traditional A-C_i curve. Instead of ramping CO_2 to specific concentrations and giving the leaf time to acclimate (as is done for traditional A-C_i measurements), RACiR involves continuously ramping CO_2 and taking measurements every 2 s, so that the instantaneous response to CO_2 changes are measured in their non-steady-state form. Using this new method provides reliable estimates of J_{max} and V_{cmax} [29,46]. However, other parameter estimates derived from this approach may be less comparable to estimates from traditional methodology [29,46,47].

We measured RACiR curves, using a LI-6800 Portable Photosynthesis System equipped with the Multiphase Flash Fluorometer chamber (LI-COR, Lincoln, Nebraska, USA) as described in Stinziano *et al.* [29] on the newest fully open leaf of an individual plant or, for plants with very small leaves, the youngest cluster of leaves. We took these measurements on days with full sun (mean ambient PAR = 1452, s.d. =

288 µmol m^{-2} s^{-1}), between 07.00 and 11.00 Pacific Standard Time. The RACiR measurement comprises two separate measurements: (i) a data curve—for which CO_2 is ramped while a leaf is in the chamber and (ii) an empty curve—for which CO_2 is ramped with no leaf in the chamber. The empty chamber curve is used to differentiate between the rate of CO_2 accumulation in the chamber and the real change in the photosynthetic rate of the leaf. According to Stinziano *et al*. [29], these empty curves should be collected periodically throughout the data collection—to account for possible environmental effects on the accumulation of CO_2 throughout the day. We took at least two empty ramp measurements per morning. We used the following settings for ramping: CO_2 ramped from 10 to 1010 ppm, temperature leaf = 20 C, light = 1500 µmol m^{-2} s^{-1}. Following the protocol developed in [29], we calibrated our data curves with the empty curves closest in time to each leaf measurement. For some species with small or irregular leaf shapes, leaf tissue did not completely cover the surface of the LI-6800 chamber. As noted below (see Functional traits), we measured the surface area of the leaf that could fit inside the chamber, we then used custom R scripts to calculate a corrected set of photosynthetic values, before fitting the curves. We used the *plantecophys* R package [48] to estimate the traits (J_{max} and V_{cmax}) from our calibrated curves using the bilinear fitting method. Prior to fitting curves, we thinned our data, keeping one in 15 observations to reduce the potential effect of temporal autocorrelation in the fitting of the RACiR data (note, however, J_{max} and V_{cmax} remain fairly constant for a wide variety of thinning intervals; electronic supplementary material, figure S4). We also manually checked our dataset to remove J_{max} and V_{cmax} estimates that were derived from poor quality data.

(c) Functional traits

After measuring a RACiR curve, the leaf (or leaves) that was sampled was clipped from the plant and placed in a resealable bag to prevent desiccation and stored in an ice-filled cooler overnight. We scanned each leaf (at 300 DPI, using a Perfection V750 PRO Epson flatbed scanner) and calculated the total leaf area as well as the leaf area inside the chamber during our RACiR measurement using ImageJ [49]. We measured leaf wet mass using a Mettler Toledo B154 analytical balance. After these measurements were taken, we placed the leaves in a drying oven at 60°C for 48 h and then measured dry mass. Dried leaf tissue was sent to the Analytical Chemical Services Laboratory (at the BC Ministry of Environment and Climate Change Strategy) for combustion analysis to obtain leaf nitrogen and carbon content per unit mass. Nitrogen and carbon contents were converted from per unit mass to per unit area basis, by multiplying the former by LMA (e.g. $N_{area} = N_{mass} \times LMA$).

(d) Phylogenetic and statistical analyses

We used the time-calibrated megaphylogeny from Zanne *et al*. [9] for all of the following phylogenetic analyses. We pruned the tree (available from: https://datadryad.org/stash/dataset/doi:10.5061/dryad.63q27) to include only the species present in our macroevolutionary common garden as tips on the tree. To facilitate cross-trait comparisons, our complete trait dataset is made up of 111 species, in which every species has a measurement for each trait.

(i) Models of trait divergence through time

We used plots of trait divergence through time to assess broad patterns of trait divergence. Following the approach of Uyeda *et al*. [1], we estimated the divergence in trait values between each species pair in our dataset for each of the traits we measured (J_{max}, V_{cmax}, leaf area, leaf mass, N_{area} and C_{area}). Divergence is measured as the log difference between two trait values (i.e. $\ln(X_1) - \ln(X_2)$, where X_1 and X_2 are the means measurements of a species pair), standardized by their dimensionality (i.e. whether these are mass, area or linear based measurements); this allows us a measurement-scale independent way to visually compare divergences between different traits [1]. We plotted these divergence values against the divergence time between species (i.e. the age of their most recent common ancestor) as estimated from the node ages of the phylogenetic tree [9]. To quantify the relationship between phylogenetic distance and trait divergence, we fit an Ornstein-Uhlenbeck (OU, [31]) process model to the comparative data using the fitContinuous function in the R package *geiger* [50]. OU models depict evolution as a balance between divergence and selection towards an evolutionary optimum. Specifically, the per unit time change in mean phenotypic value Δz is equal to

$$\Delta z = -\alpha(z - \theta) + \sigma dW$$

where α is the strength of attraction towards the optimum θ, and σ is the rate of divergence according to a continuous-time Wiener process dW. We estimated the maximum-likelihood value for all parameters using the fitContinuous function in the R package *geiger* [50]. In these model fits, measures of leaf area and mass were log transformed, and measurement error for all traits was incorporated by using the variance of our species sample of three leaves. We then calculated the half-life of the evolutionary process [32] as $\ln(2)/\alpha$.

(ii) Phylogenetically informed regressions

To estimate the value of functional traits (LMA, N_{area} and C_{area}) for predicting metabolic ones (J_{max} and V_{cmax}) in the context of phylogenetically structured data, we use Pagel's lambda as an evolutionary model and fit two phylogenetic linear regressions with the *phylolm* [51] package in R. We switch to using LMA here, rather than the raw trait values for area and mass, because traits that capture variation in the proportional allocation of resources (as LMA does) within a leaf are more commonly applied in this predictive context [36,52].

(iii) Rate of trait evolution (PICs)

For each trait (J_{max}, V_{cmax}, LMA, N_{area} and C_{area}) we estimate phylogenetic-independent contrasts (PICs) [39] for all nodes, using the R package *ape* [53]. The log of the absolute value of these contrasts estimates the rate of evolution of that trait along the phylogeny [40]. We then test whether rates of evolution of different traits (as measured by the log of the absolute value of their PIC) are correlated with each other using Pearson' product-moment correlation.

Data accessibility. All original data are available from the Dryad Digital Repository: https://doi.org/10.5061/dryad.9zw3r22f0 [54]. The code used for cleaning and analysing this dataset is available at https://github.com/bnetobradley/metamorphylo.

Authors' contributions. B.N.: conceptualization, data curation, formal analysis, writing-original draft, writing-review and editing; C.M.: conceptualization, formal analysis, writing-original draft, writing-review and editing; J.W.: conceptualization, writing-original draft, writing-review and editing; M.P.: conceptualization, formal analysis, writing-original draft, writing-review and editing

All authors gave final approval for publication and agreed to be held accountable for the work performed therein.

Competing interests. We declare we have no competing interests

Funding. This work was supported by NSERC Canada Discovery Grants to M.W.P. and J.W. M.W.P. was also supported by a Canada Research Chair (Tier II) and a CFI John R. Evans Leaders Fund Grant. C.D.M. was supported by start-up funds from the University of Hawai'i. B.M.N.B. was supported by a NSERC CGS-M Fellowship. This is publication number 117 from the School of Life Sciences, University of Hawai'i at Mānoa.

Acknowledgements. We thank the UBC and VanDusen Botanical Gardens, and in particular the support of Cynthia Sayre, Daniel Mosquin, Ben Stormes and Laura Caddy. We thank Varoon Pornsinsiriruk and Léonard Dekens for assistance with data collection and fieldwork, and Diane Srivastava for the use of her laboratory truck. We thank Josef Uyeda, Amy Angert, Sean Michaletz and members of the Pennell and Whitton labs for discussion of these ideas.

References

1. Uyeda JC, Hansen TF, Arnold SJ, Pienaar J. 2011 The million-year wait for macroevolutionary bursts. *Proc. Natl Acad. Sci. USA* **108**, 15 908–15 913. (doi:10.1073/pnas.1014503108)
2. Harmon LJ *et al.* 2010 Early bursts of body size and shape evolution are rare in comparative data. *Evolution* **64**, 2385–2396.
3. Dakin R, Segre PS, Straw AD, Altshuler DL. 2018 Morphology, muscle capacity, skill, and maneuvering ability in hummingbirds. *Science* **359**, 653–657. (doi:10.1126/science.aao7104)
4. Houle D, Bolstad GH, van der Linde K, Hansen TF. 2017 Mutation predicts 40 million years of fly wing evolution. *Nature* **548**, 447–450. (doi:10.1038/nature23473)
5. Weber MG, Agrawal AA. 2012 Phylogeny, ecology, and the coupling of comparative and experimental approaches. *Trends Ecol. Evol.* **27**, 394–403. (doi:10.1016/j.tree.2012.04.010)
6. Fagan WF, Pearson YE, Larsen EA, Lynch HJ, Turner JB, Staver H, Noble AE, Bewick S, Goldberg EE. 2013 Phylogenetic prediction of the maximum per capita rate of population growth. *Proc. Biol. Sci.* **280**, 20130523. (doi:10.1098/rspb.2013.0523)
7. Díaz S, Purvis A, Cornelissen JHC, Mace GM, Donoghue MJ, Ewers RM, Jordano P, Pearse WD. 2013 Functional traits, the phylogeny of function, and ecosystem service vulnerability. *Ecol. Evol.* **3**, 2958–2975. (doi:10.1002/ece3.601)
8. Cornwell WK *et al.* 2014 Functional distinctiveness of major plant lineages. *J. Ecol.* **102**, 345–356. (doi:10.1111/1365-2745.12208)
9. Zanne AE *et al.* 2014 Three keys to the radiation of angiosperms into freezing environments. *Nature* **506**, 89–92. (doi:10.1038/nature12872)
10. Edwards EJ, Smith SA. 2010 Phylogenetic analyses reveal the shady history of C4 grasses. *Proc. Natl Acad. Sci. USA* **107**, 2532–2537. (doi:10.1073/pnas.0909672107)
11. Muir CD. 2015 Making pore choices: repeated regime shifts in stomatal ratio. *Proc. Biol. Sci.* **282**, 20151498.
12. Mason CM, Donovan LA. 2015 Evolution of the leaf economics spectrum in herbs: evidence from environmental divergences in leaf physiology across *Helianthus* (Asteraceae). *Evolution* **69**, 2705–2720. (doi:10.1111/evo.12768)
13. Jordan GJ, Carpenter RJ, Holland BR, Beeton NJ, Woodhams MD, Brodribb TJ. 2020 Links between environment and stomatal size through evolutionary time in Proteaceae. *Proc. Biol. Sci.* **287**, 20192876. (doi:10.1098/rspb.2019.2876)
14. von Caemmerer S. 2000 *Biochemical models of leaf photosynthesis*. Clayton South, Australia: CSIRO Publishing. (doi:10.1071/9780643103405)
15. Farquhar GD, von Caemmerer S, Berry JA. 1980 A biochemical model of photosynthetic CO_2 assimilation in leaves of C_3 species. *Planta* **149**, 78–90. (doi:10.1007/BF00386231)
16. Walker AP *et al.* 2014 The relationship of leaf photosynthetic traits — V_{cmax} and J_{max} — to leaf nitrogen, leaf phosphorus, and specific leaf area: a meta-analysis and modeling study. *Ecol. Evol.* **4**, 3218–3235. (doi:10.1002/ece3.1173)
17. Nadal M, Flexas J. 2019 Variation in photosynthetic characteristics with growth form in a water-limited scenario: implications for assimilation rates and water use efficiency in crops. *Agric. Water Manage* **216**, 457–472.
18. Sharkey TD, Bernacchi CJ, Farquhar GD, Singsaas EL. 2007 Fitting photosynthetic carbon dioxide response curves for C_3 leaves. *Plant Cell Environ.* **30**, 1035–1040. (doi:10.1111/j.1365-3040.2007.01710.x)
19. Gago J, Carriquí M, Nadal M, Clemente-Moreno MJ, Coopman RE, Fernie AR, Flexas J. 2019 Photosynthesis optimized across land plant phylogeny. *Trends Plant Sci.* **24**, 947–958. (doi:10.1016/j.tplants.2019.07.002)
20. Carriquí M *et al.* 2015 Diffusional limitations explain the lower photosynthetic capacity of ferns as compared with angiosperms in a common garden study. *Plant Cell Environ.* **38**, 448–460. (doi:10.1111/pce.12402)
21. Lusk CH, Wright I, Reich PB. 2003 Photosynthetic differences contribute to competitive advantage of evergreen angiosperm trees over evergreen conifers in productive habitats. *New Phytol.* **160**, 329–336. (doi:10.1046/j.1469-8137.2003.00879.x)
22. Flexas J, Carriquí M. 2020 Photosynthesis and photosynthetic efficiencies along the terrestrial plant's phylogeny: lessons for improving crop photosynthesis. *Plant J.* **101**, 964–978. (doi:10.1111/tpj.14651)
23. Knight CA, Vogel H, Kroymann J, Shumate A, Witsenboer H, Mitchell-Olds T. 2006 Expression profiling and local adaptation of *Boechera holboellii* populations for water use efficiency across a naturally occurring water stress gradient. *Mol. Ecol.* **15**, 1229–1237. (doi:10.1111/j.1365-294X.2006.02818.x)
24. Keller SR, Soolanayakanahally RY, Guy RD, Silim SN, Olson MS, Tiffin P. 2011 Climate-driven local adaptation of ecophysiology and phenology in balsam poplar, *Populus balsamifera* L. (Salicaceae). *Am. J. Bot.* **98**, 99–108. (doi:10.3732/ajb.1000317)
25. Bunce JA. 2000 Acclimation of photosynthesis to temperature in eight cool and warm climate herbaceous C_3 species: temperature dependence of parameters of a biochemical photosynthesis model. *Photosynth. Res.* **63**, 59–67. (doi:10.1023/A:1006325724086)
26. Gratani L. 2014 Plant phenotypic plasticity in response to environmental factors. *Adv. Bot.* **2014**, 1–17. (doi:10.1155/2014/208747)
27. Gago J, Daloso D de M, Figueroa CM, Flexas J, Fernie AR, Nikoloski Z. 2016 Relationships of leaf net photosynthesis, stomatal conductance, and mesophyll conductance to primary metabolism: a multispecies meta-analysis approach. *Plant Physiol.* **171**, 265–279. (doi:10.1104/pp.15.01660)
28. Wang D, Heckathorn SA, Wang X, Philpott SM. 2012 A meta-analysis of plant physiological and growth responses to temperature and elevated CO_2. *Oecologia* **169**, 1–13. (doi:10.1007/s00442-011-2172-0)
29. Stinziano JR, Morgan PB, Lynch DJ, Saathoff AJ, McDermitt DK, Hanson DT. 2017 The rapid A-C_i response: photosynthesis in the phenomic era. *Plant Cell Environ.* **40**, 1256–1262. (doi:10.1111/pce.12911)
30. Niinemets U. 2007 Photosynthesis and resource distribution through plant canopies. *Plant Cell Environ.* **30**, 1052–1071. (doi:10.1111/j.1365-3040.2007.01683.x)
31. Hansen TF. 1997 Stabilizing selection and the comparative analysis of adaptation. *Evolution* **51**, 1341–1351. (doi:10.1111/j.1558-5646.1997.tb01457.x)
32. Hansen TF, Orzack SH. 2005 Assessing current adaptation and phylogenetic inertia as explanations of trait evolution: the need for controlled comparisons. *Evolution* **59**, 2063–2072. (doi:10.1111/j.0014-3820.2005.tb00917.x)
33. Uyeda JC, Pennell MW, Miller ET, Maia R, McClain CR. 2017 The evolution of energetic scaling across the vertebrate tree of life. *Am. Nat.* **190**, 185–199. (doi:10.1086/692326)
34. Avaria-Llautureo J, Hernández CE, Rodríguez-Serrano E, Venditti C. 2019 The decoupled nature of basal metabolic rate and body temperature in endotherm evolution. *Nature* **572**, 651–654. (doi:10.1038/s41586-019-1476-9)
35. Muir CD, Thomas-Huebner M. 2015 Constraint around quarter-power allometric scaling in wild tomatoes (*Solanum* sect. *Lycopersicon*; Solanaceae). *Am. Nat.* **186**, 421–433. (doi:10.1086/682409)
36. Wright IJ *et al.* 2004 The worldwide leaf economics spectrum. *Nature* **428**, 821–827. (doi:10.1038/nature02403)
37. Osnas JLD, Lichstein JW, Reich PB, Pacala SW. 2013 Global leaf trait relationships: mass, area, and the leaf economics spectrum. *Science* **340**, 741–744. (doi:10.1126/science.1231574)
38. Uyeda JC, Bone N, McHugh S, Rolland J, Pennell MW. 2021 How should functional relationships be evaluated using phylogenetic comparative methods? A case study using metabolic rate and body

temperature. *Evolution* **75**, 1097–1105. (doi:10.1111/evo.14213)

39. Felsenstein J. 1985 Phylogenies and the comparative method. *Am. Nat.* **125**, 1–15. (doi:10.1086/284325)
40. Garland T, Harvey PH, Ives AR. 1992 Procedures for the analysis of comparative data using phylogenetically independent contrasts. *Syst. Biol.* **41**, 18–32. (doi:10.1093/sysbio/41.1.18)
41. Agrawal AA. 2020 A scale-dependent framework for trade-offs, syndromes, and specialization in organismal biology. *Ecology* **101**, e02924.
42. Cantalapiedra JL, Fitzjohn RG, Kuhn TS, Fernández MH, DeMiguel D, Azanza B, Morales J, Mooers AØ. 2014 Dietary innovations spurred the diversification of ruminants during the Caenozoic. *Proc. R. Soc. B* **281**, 20132746. (doi:10.1098/rspb.2013.2746)
43. Yiotis C, McElwain JC. 2019 A novel hypothesis for the role of photosynthetic physiology in shaping macroevolutionary patterns. *Plant Physiol.* **181**, 1148–1162. (doi:10.1104/pp.19.00749)
44. Rogers A. 2014 The use and misuse of $V_{c,max}$ in Earth System Models. *Photosynth. Res.* **119**, 15–29. (doi:10.1007/s11120-013-9818-1)
45. Ort DR *et al.* 2015 Redesigning photosynthesis to sustainably meet global food and bioenergy demand. *Proc. Natl Acad. Sci. USA* **112**, 8529–8536. (doi:10.1073/pnas.1424031112)
46. Stinziano JR, McDermitt DK, Lynch DJ, Saathoff AJ, Morgan PB, Hanson DT. 2019 The rapid A/Ci response: a guide to best practices. *New Phytol.* **221**, 625–627. (doi:10.1111/nph.15383)
47. Taylor SH, Long SP. 2019 Phenotyping photosynthesis on the limit—a critical examination of RACiR. *New Phytol.* **221**, 621–624. (doi:10.1111/nph.15382)
48. Duursma RA. 2015 Plantecophys—an R package for analysing and modelling leaf gas exchange data. *PLoS ONE* **10**, e0143346. (doi:10.1371/journal.pone.0143346)
49. Schneider CA, Rasband WS, Eliceiri KW. 2012 NIH Image to ImageJ: 25 years of image analysis. *Nat. Methods* **9**, 671–675. (doi:10.1038/nmeth.2089)
50. Pennell MW, Eastman JM, Slater GJ, Brown JW, Uyeda JC, FitzJohn RG, Alfaro ME, Harmon LJ. 2014 geiger v2.0: an expanded suite of methods for fitting macroevolutionary models to phylogenetic trees. *Bioinformatics* **30**, 2216–2218. (doi:10.1093/bioinformatics/btu181)
51. Ho LsT, Ané C. 2014 A linear-time algorithm for Gaussian and non-Gaussian trait evolution models. *Syst. Biol.* **63**, 397–408. (doi:10.1093/sysbio/syu005)
52. Reich PB. 2014 The world-wide 'fast–slow' plant economics spectrum: a traits manifesto. *J. Ecol.* **102**, 275–301. (doi:10.1111/1365-2745.12211)
53. Paradis E, Claude J, Strimmer K. 2004 APE: analyses of phylogenetics and evolution in R language. *Bioinformatics* **20**, 289–290. (doi:10.1093/bioinformatics/btg412)
54. Neto-Bradley BM, Muir CD, Whitton J, Pennell MW. 2021 Data from: Phylogenetic history of vascular plant metabolism revealed using a macroevolutionary common garden. Dryad Digital Repository. (https://doi.org/10.5061/dryad.9zw3r22f0)